PINCH: An Adversarial Extraction Attack Framework for Deep Learning Models

William Hackett[1], Stefan Trawicki[1], Zhengxin Yu[1], Neeraj Suri[1,2], and Peter Garraghan[1,2]

[1]Lancaster University
[2]Mindgard

Abstract

Adversarial extraction attacks constitute an insidious threat against Deep Learning (DL) models in-which an adversary aims to steal the architecture, parameters, and hyper-parameters of a targeted DL model. Existing extraction attack literature have observed varying levels of attack success for different DL models and datasets, yet the underlying cause(s) behind their susceptibility often remain unclear, and would help facilitate creating secure DL systems. In this paper we present *PINCH*: an efficient and automated extraction attack framework capable of designing, deploying, and analyzing extraction attack scenarios across heterogeneous hardware platforms. Using PINCH, we perform extensive experimental evaluation of extraction attacks against 21 model architectures to explore new extraction attack scenarios and further attack staging. Our findings show (1) *key extraction characteristics* whereby particular model configurations exhibit strong resilience against specific attacks, (2) even partial extraction success enables further staging for other adversarial attacks, and (3) equivalent stolen models uncover differences in expressive power, yet exhibit similar captured knowledge.

1 Introduction

Deep Learning (DL) has become a critical technology supporting a growing diversity of applications. However, the successful deployment and execution of DL models is threatened by cyber attacks occurring within systems [4, 16, 25, 58], compromising DL model integrity, privacy, and confidentiality [64]. A particularly damaging threat against DL models are *extraction attacks* (also known as *model stealing*). Extraction attacks occur when an adversary attempts to extract fundamental characteristics of a target DL model (architecture, parameters, hyper-parameters) [63, 69] to reconstruct an identical or highly similar DL model [30]. Such attacks result in information leakage, digital IP theft, and enable further DL model attacks to be staged [25, 62, 69].

Extensive studies of DL model extraction attacks have been conducted to understand and mitigate their impact [9, 64].

However these studies have predominately been performed with isolated attacks, each leveraging distinctive threat models and deployment scenarios with different DL model types, datasets, and hardware platforms. Given that extraction attacks yield varying degrees of success when exposed to different DL model types and datasets [25, 58, 63, 68], it is necessary to study extraction attacks across a multitude of deployment scenarios to determine whether there exist common associations between extraction attack success, DL model characteristics and platform hardware properties.

Attaining such knowledge is constrained by the overwhelmingly high technical effort (and time) required to understand, implement and evaluate the large number of unique extraction attacks, platforms and DL model architectures in existence. This is because current studies are bespokely designed to operate for a targeted or small sub-set of deployment scenarios (e.g. a single hardware platform or DL model architecture) [24, 25, 58]. Whilst this approach is effective to demonstrate extraction attack feasibility, it is not possible to study attack effectiveness and generalizability without extensive re-designing and engineering of attacks to operate within different operational scenarios [32, 37, 59].

Extensive progress has been made to create extraction attack frameworks to alleviate the complexity of re-implementing attacks and providing configurable attack scenarios [29, 36, 43]. However, such frameworks exhibit limitations towards studying generalizable features of extraction attacks, as current proposed frameworks provide discrete approaches towards extraction, typically only implementing attacks within one area of the DL system attack surface and targeting specific model characteristics [36, 69]. Additionally, current frameworks are often limited to executing smaller (often bespoke) models and datasets, unable to evaluate larger models and complex dataset pairings deployed within the modern DL landscape.

To tackle limitations of existing work, we present PINCH: an efficient and automated extraction attack framework capable of deploying a large number of DL models, attacks, and deployment environments in a generalizable manner. Our frame-

work performs (1) *dynamic framework-independent model loading and training* via transfer learning and curated AI deployment repositories, with (2) configuration of attacks encapsulated as *attack scenarios*, and (3) *experiment automation* for recording and reporting.

PINCH is capable of automated attack execution that extracts DL model characteristics utilizing multiple areas of the DL system attack surface, enabling exploration of scenarios not examined within contemporary literature, and provides support for unexplored adversarial attack staging. We demonstrate the effectiveness of PINCH by empirically evaluating extraction scenarios across different state-of-the-art extraction attack types [24, 25, 46] when exposed to various DL model architectures, datasets, and hardware/software environments. Our work makes the following contributions:

- **PINCH**: An end-to-end automated adversarial attack framework capable of efficiently executing extraction attack scenarios and enabling detailed evaluation across a variety of model families, architectures, datasets, and hardware platforms (Section 5).

- **Key extraction characteristics**: Through extensive experimentation of hundreds of unique extraction attack scenarios, we have identified key extraction attack characteristics that affect success spanning model architecture, and dataset complexity, and hardware (Section 7).

- **Further attack staging**: We demonstrate the feasibility of adversarial attack staging. Discovering it is possible to launch successful model inversion attacks on DL models created from partially successful extraction attacks, additionally uncovering limitations in existing methods for measuring DL model similarity for denoting attack success (Section 7.4).

- **Stolen model equivalency**: We have identified that stolen models can exhibit equivalent target model performance, yet exhibit similar captured knowledge while being composed of uniquely different DL model characteristics (Section 8.3).

2 Background

2.1 Deep Learning Systems

Deep Learning (DL) is a sub-field of *Machine Learning (ML)*, which uses multiple processing layers to learn representations from input data with multiple levels of abstraction [35]. *DL models* are represented by *Deep Neural Networks* (DNNs); collections of *Operators* (Convs, MaxPool, ReLU, etc.), specialized programs designed for performing actions on tensors, grouped into *Layers*. A DNNs operator layers are selected and organized based on desired *architecture* best suited for different applications, *e.g.*, Convolutional Neural Networks
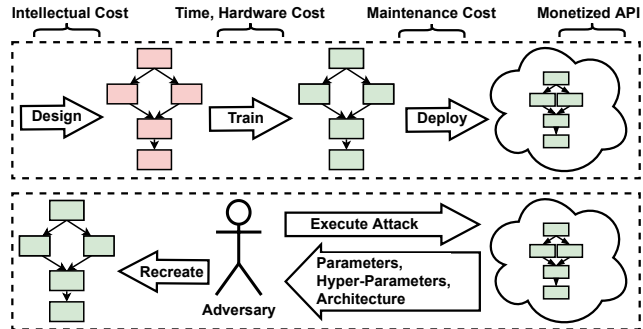

Figure 1: **Overview of extraction attack process**. Deep Learning models comprising of architecture, parameters and hyper-parameters can be be stolen via extraction attacks.

(CNNs) for image classification, and Long Short-Term Memory (LSTM) for time-series data analysis. DL models leverage accelerator devices such as *Graphics Processing Units* (GPUs) that enable parallel execution of operators, hastening the training process [19], as well as performing faster model inference. A *Deep Learning System (DL system)* provides, CPU, accelerators and the accompanying software (ML frameworks, libraries) to perform DL model training and inference.

DL systems have been widely adopted throughout both industry and research, providing considerable acceleration to the creation of cutting-edge DL models capable of performing tasks unknown to previous generational systems [53]. The widespread usage of such systems has lead to increasing concern of privacy and security related issues surrounding deployed DL models. The increased data and sophistication present in DL models has made DL systems a target for *adversarial attacks*, aiming to perform attacks spanning model evasion [3], poisoning [57], as well as extract sensitive and confidential data [4, 62, 69]. The concern raised from the existence of such attacks has prompted extensive research to understand adversarial attacks [4, 27, 62], and protection against successful attack execution [20, 64].

2.2 Model Extraction

Model extraction, also referred to as *model stealing*, is a set of adversarial attacks that extract fundamental *characteristics* of a DL model: its architecture, parameters and hyper-parameters (Figure 1). A *stolen model* is created using extraction techniques to collect information leakage (model characteristics) via access to a target DL model or its underlying DL system, and *recreating* a copy of the *target model* [25, 63, 69]. A stolen model can be used for further attacks [58] or designing a replica model with similar performance [58, 69].

Extraction techniques. DL models can be stolen across a wide range of attack surfaces covering various areas of the DL system stack. For instance, an adversary can perform

prediction API attacks by obtaining predictions on input feature vectors to train a local substitute model [58, 67, 68], or a side-channel attack by extracting information leakage from Peripheral Component Interconnect Express (PCIe) traffic. Many works have demonstrated that system operation (*i.e.*, timing, power usage, computation, cache) can be exploited to infer the underlying operators of the DL model and used to perform model extraction [24, 25, 63]. Based on *MITRE ATLAS (MA)*, attacks have different numbers of intermediate stages depending on their *tactics* and their enabling *techniques* [12]. (1) *Initial Access*, where the adversary prepares the environment such as deploying spy kernels and monitoring code [25, 69]. (2) *Attack Staging*, wherein preliminary attacks are launched to gather DL model system and model information [25]. (3) *Exfiltration*, primarily the deployment of API attacks, potentially using previously gathered information from attack staging. [42, 63, 69].

Model recreation. Recreation focuses on training a model, either uninitialized or pre-trained, that provides an architecture and weights [25, 67] with the intention of replicating a target model by leveraging collected information leakage of DL model characteristics. Extracted target model characteristics can be acquired using a number of adversarial attacks, such as a training set created from synthetic or ground truth inputs paired with confidence values or labels gained from a prediction API attack [58, 67, 69]. It is feasible for sophisticated approaches using side-channels to observe DL system traffic to infer DL model characteristics [25, 63, 69]. Using gathered metrics, GPU kernels mappings and inference inputs and outputs enable the creation of a dataflow graph representing model architecture layout. The complexity of model recreation can be vast due to the possible combinations of ML frameworks, compute libraries, model architectures, among other variables that can be partially and entirely unknown to an adversary when attacking a DL system.

Consequence. Failure to defend against extraction attacks can compromise the integrity, privacy and confidentiality of the DL system. System integrity can be compromised during attack preparation and execution, with the potential backdoors created for future access [55]. Data privacy is degraded via stolen model characteristics being exploited to stage further attacks that extract training data information [21, 58]. Furthermore, the confidentiality of the DL model is compromised since adversaries have access to model characteristics, therefore allowing adversaries to reverse engineer and steal confidential data, such as the training dataset.

2.3 Challenges in Extraction Attack Research

In model extraction literature, a number of studies have demonstrated the feasibility and practicality of extraction attacks against DL models [46, 58, 69]. However these studies are predominately performed with isolated attacks targeting one DL model characteristic, leveraging distinctive threat models, and bespoke deployment scenarios with different DL types [25, 58, 63, 68]. This is problematic given the evolving DL landscape of extraction scenarios whereby current extraction attack implementations are obsolete when paired with state-of-the-art DL types [37, 59], and DL systems [32, 44].

From extraction attack literature, it is observable that extraction attacks yield varying degrees of success when exposed to different DL model types and datasets [58, 69]. However, current extraction attacks lack the generalizability required to execute attacks across different extraction scenarios. Exploring common associations is challenging due to the technical effort required to conduct attacks across attack scenarios in software and hardware heterogeneous DL systems. Understanding the associations attributed to DL types, datasets, and deployment scenarios can greatly benefit the fundamental understanding towards varying extraction success observed in literature [25, 58, 63, 68]. Therefore, given the vast amount of deployment scenarios it is necessary to alleviate the limitations present within current work, and further study the common associations within extraction attacks across a multitude of deployment scenarios, DL types, and datasets.

PINCH targets the capability of an efficient and automated extraction attack framework able to deploy and evaluate DL model security across heterogeneous DL systems and extraction attack scenarios with design goals of: (1) *Generalizability*, providing a unified platform for the hardware and software used in DL system deployments, and for the attacks that target them. (2) *Configuration & Automation*, providing a machine independent system to define an attack scenario and deploy it for repeatable experimentation at scale.

3 Threat Model

The objective of a DL model is to map an input to a provided classification. Given an input, the model propagates through its operators to output a vector of probabilities denoting the confidence of classification associated to the input. The threat models underpinning extraction attacks in this paper are categorized into three aspects: *Model knowledge*, *DL System Environment knowledge* and access to the *Auxiliary dataset*.

Model knowledge. We consider two access types *observed* (M_o) and *hidden* (M_h). With *observed* knowledge, an adversary has access to sufficient[1] information of the target model (architecture, parameters) to infer its model characteristics. With *hidden* knowledge, adversary access is limited to API calls to the target model (query, data output from model), with attacks [18] assuming that the model architecture is already known to construct a shadow model. *Hidden* knowledge encompasses scenarios whereby a target model is accessed via external API calls commonly found in Machine Learning as a Service (MLaaS). *Observed* knowledge encapsulates informa-

---

[1]We deliberately use the term "sufficient" as certain attacks only require a limited sub-set of target model information to succeed.

tion leakage of target model characteristics via attacks such as bus snooping, and side-channel.

DL system knowledge. Knowledge pertaining the DL system environment is used to infer DL model characteristics. Two types of knowledge are considered for the DL environment: *partial (S_p)*, and *none (S_n)*. Types denote the adversaries knowledge associated with the target DL environment the target model is executing upon. This includes knowledge regarding DL framework, GPU accelerators, and CPU devices. *Partial* knowledge of the environment enables an adversary to have direct or indirect knowledge about the DL environment, for example, knowing the type of CPU (Intel, AMD), or GPU (Nvidia, AMD). *None* states the adversary has no information regarding the DL environment, and encompasses scenarios whereby an adversary may have no, or not need any knowledge about the DL system.

Auxiliary dataset. Depending on the type of attack, the adversary may require an auxiliary dataset to perform their attack. We consider two scenarios in decreasing order of adversarial "strength": (1) *Partial (D_p)* where an adversary has some knowledge of target dataset and therefore can obtain parts of the target dataset (e.g. via public knowledge, or staging previous attacks). (2) *No dataset (D_n)* whereby the adversary has no information regarding the dataset. We assume the attacker has access to open source datasets commonly provided by DL libraries or online repositories [13, 39, 65].

Overall scenarios. Considering the model knowledge, DL environment knowledge, and auxiliary dataset a total of 8 distinctive threat models are possible. In the rest of the paper we focus on two: (M_h, S_n, D_p), and (M_o, S_p, D_n). As the scenarios are tailored to extraction attacks 6 scenarios are omitted due to their indifference to extraction success.

4 Extraction Attacks

4.1 KnockOffNets (KON)

KnockOffNets (KON) [46] is an inference attack whereby an adversary undergoes inference upon a target model by querying with a set of images randomly sampled from a *query set* to steal target model parameters and recreate a stolen model. All predictions made by the target model are combined into a new *stolen dataset* containing the previously queried images and stolen prediction confidence values or label pairs. The stolen dataset is then used to reconstruct a new model via a training recreation technique, in which an untrained model of the same architecture as the target is trained on stolen dataset until the desired similarity to the target is reached. The adversary's intention is for the stolen model to be equivalent when compared to the target model within the targets task.

KON leverages the assumptions (M_h, S_n, D_p). The adversary has hidden knowledge access to the target model while being capable of performing inference requests with queries, and does not assume any rate limiting or other inference coun-

termeasures associated with the target model. Inference extraction attacks only use the API to access the DL target model which is abstracted away from the underlying DL system, meaning no DL system knowledge is required. The adversary has partial auxiliary dataset knowledge about the underlying target model architecture and training dataset used to therefore establish a query set to be used during the attack.

4.2 DeepSniffer (DS)

DeepSniffer (DS) focuses on utilizing leaky information from the GPU to infer target model architecture [25]. DS captures 4 kernel metrics during operator execution; *execution time (Exe_{Lat}), read volume (R_V), write volume (W_V), and I/O output volume (I_V / O_V)*, to understand the relationship between operators and variance of metrics. From this relationship, DS can infer one of seven operators within a target model architecture; *Conv, ReLU, BN, Pool, Concat, Add, and FC kernels* via a pre-trained DL model trained upon previous examples leaked by the GPU, called the *DS model*. There are two attack stages: (1) *Attack Staging*: Whereby DS gathers required GPU metrics during target model execution. (2) *Exfiltration:* DS uses the gathered data to undergo architecture prediction via a previously trained DS model.

We make the following assumptions (M_o, S_p, D_n): The adversary observes knowledge about the target model via architectural hints exposed within the GPU that the target model is executing upon. We assume the adversary has partial knowledge of the DL system, and the capability to access low level system functionality including capturing stream of memory and PCI metrics for CPU/Memory $\rightarrow$ GPU communication of the target model to infer kernel metrics through GPU profiling tools such as NVPROF [14]. Knowledge pertaining to the target models ML framework is also considered due to the attack staging requirements. Finally, the adversary must be capable of performing inferences upon the target model. Auxiliary dataset knowledge is not required as activating the networks operators is the focus, not the models prediction, for which data outside the auxiliary set can be used.

4.3 DeepRecon (DR)

DeepRecon (DR) [24] is a side-channel extraction attack that gathers target model architecture information by using information leakage from a device's CPU L3 cache. DeepRecon extracts eight DL operators (*Conv, MatMul, Softmax, Relu, MaxPool, AveragePool, Merge & Bias*) by associating them with symbols from the target model framework binary and identify their execution by starting a co-located programme to monitor L3 cache. In the case of a CPU attack, Flush+Reload [66] is used to flush the CPUs L3 cache to observe which symbols repopulate the cache on the assumption that frequently occurring symbols belong to a target executing DL process. Dimensional reduction techniques, such as Principle Com-

ponent Analysis (PCA), can then be used to cluster gathered symbols during a model execution, making it possible for an adversary to infer the architecture of a model by comparing reduced dimensions to that of other known models.

DR leverages the assumptions (M_o, S_p, D_n): The adversary has observed model and partial DL system knowledge whereby it is known that targeted systems are vulnerable to Flush+Reload. Similarly to DeepRecon, auxiliary dataset knowledge is not required. It is assumed that: (1) An adversary is capable of launching co-located user-level processes on the host of the target model. (2) The target and attacking processes use the same DL framework binaries, to associate symbols with DL operators. (3) The adversary knows which CPU architecture is in use, as Flush+Reload is an Intel exploit.

4.4 MiFace (Inversion Attack)

To demonstrate the frameworks ability to enable further attacks to be staged upon extracted models, we implemented the *MiFace* model inversion attack by Fredrikson *et al.* [17]. Model inversion is a privacy violating attack whereby an adversary with access to an inference API seeks to reconstruct a representative example from each class within the DL model. The consequence of such an attack is the ability for images of trained classes within a model to be extracted. For each class within the target model, the adversary performs back-propagation over target model parameters to optimize the input sample so that the corresponding class posterior exceeds an established threshold. An input sample can be a randomly generated image, or another initialization technique denoted via an adversaries knowledge of the DL model.

Model inversion leverages the assumptions (M_h, S_n, D_p): It is assumed that the adversary is targeting a model with hidden knowledge, requiring the capability to perform prediction queries on feature vectors targeted by an adversary. As seen previously in 4.2 and 4.3, no DL system environment knowledge is required as model inversion uses the inference API which provides abstraction from the DL systems software and hardware. Furthermore, partial knowledge of model classes is required: with a facial recognition model, the adversary indirectly knows the model responds positively to faces, and the adversary requires access to an auxiliary dataset providing input initialization values.

5 Framework Design

The objective of PINCH is to simplify and generalize the process of executing adversarial attacks, facilitating the exploration of associations between attacks, DL model characteristics, and DL systems. The framework accomplishes this by creating interfaces to standardize model inputs, data sets and software environments, providing compatibility for the execution of attacks. Additionally we enable readily reproducible configuration and automation of attack scenarios to
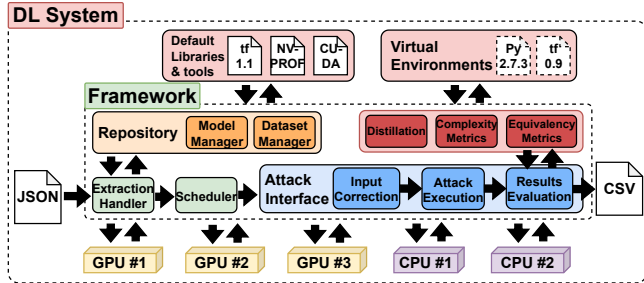

Figure 2: **Extraction framework system model and components.**

gather insights, with straightforward deployment into a DL system without coding or complex build processes. Figure 2 depicts PINCH and its five components: *Scheduler*, *Extraction Handler*, *Attack Interface*, *Model Manager*, *Results & Metrics*, and *Repositories*.

5.1 Components

User Interface. PINCH was designed for both *Command Line Interfaces (CLI)* and *Browser Interfaces (BI)*, and can readily interface with established AI/ML/DL pipelines. Internally, extraction attack scenarios are stored as JSON objects and are parsed to configure the module pipeline. Single or multi-stage scenarios are passed to the attack function and the results returned within 10 LoC in Python using the CLI. The BI was implemented using a ReactJS front end and Flask web server framework [54, 60], providing the same facilities but with GUI features, such as drop-down attack scenario configuration and generated results visualizations.

Extraction Handler. We implement the pipeline software design pattern [6] by instantiating components required for an attack scenario and having unidirectional data flow, with the *extraction handler* being the pipeline orchestrator. Given large datasets and models are I/O and memory intensive to load and unload, the extraction handler requests the dataset and model managers to begin loading resources from disk immediately when executed to reduce pipeline latency. Additionally, software environments (libraries, frameworks, interpreters) are preemptively created for a given attack to execute within, either referencing software installed on the DL system, or through the use of virtual environments. Alternative Python library versions are created and accessed using *venv* [40], creating lightweight site directories isolated from the default system packages. Attacks with more complex dependencies and build processes, such as DeepRecon, are assigned and run in a containerized environment via docker.

Scheduler. We enable multiple attack scenarios to be executed concurrently on a DL system through a scheduler. A heuristic method assesses the attacks, the currently available resources (*e.g.* GPUs and memory), and decides whether the

attacks can be ran in parallel. Once agreed, the DL frameworks are configured to use the assigned resources and attack interfaces components instantiated for each attack. Parallel compute time for KON is $\frac{1}{n}$ with n GPUs installed in the DL system, compared to linear execution. Side-channel snooping attacks are not run in parallel, as the operations of other executing attacks (*noise*) may provide unsatisfactory results.

Attack Interface. The *attack interface* creates a valid input configuration for executing a given attack scenario. As mentioned in Section 2.3, successful attack execution is highly dependent on input data being syntactically correct. The attack interface implements stub methods that manipulate the attack input from intermediate representations to the standard compatible for the attack depending on scenario. This protects from crash-stop failures caused by fragile input errors regardless of extraction attack and model architecture. The interface wraps the attack execution calls, recording queries and responses or predicted architectures, and performs attack-contextual evaluation *e.g.* calculating model extraction fidelity and similarity methods [41].

Dataset Manager. Inefficient loading techniques in existing attack frameworks makes testing contemporary datasets often exhaust system memory by attempting to load entire datasets simultaneously. This was resolved by creating a *loader* that automatically splits requested datasets into chunks and loads them progressively into memory on demand, and by limiting the retrieved dataset objects to the number of queries set to execute, rather than the entire set.

Model Manager. The model manager fulfills requests by attacks to load models, while providing for compatibility and reduced user involvement. PINCH maintains a repository consisting of online [11, 39] and local DL models and their checkpoint history. We built a server to serve models by framework, architecture, stage of training and subsets trained classes, additionally implementing automatic transfer learning capabilities [70] to: (1) train variants of existing model architectures with compatibility for new datasets, and 2) train models used in attacks on targeted subsets of a models classes.

6 Experimental Setup

Experiments consisted of studying 21 state-of-the-art DL architectures trained across four benchmark datasets, creating a total of 92 target models. These target models were exposed to three extraction attacks (see Section 4) and one model inversion attack. Complying with threat models described in Section 3, datasets are separated into an auxiliary and testing sets for fidelity comparisons.

Using PINCH, target models and corresponding dataset were automatically deployed into specific DL framework and hardware devices (Section 6.1). Next, a configured extraction attack was launched against the target model (Section 6.3) and dataset (Section 6.2). On attack completion, we used our framework to extract and collate results to analyze, research, and study extraction attacks within Sections 7 and 8.

6.1 Hardware & Software Setup

Experiments were conducted on multiple hardware platforms. KON – whose effectiveness is reported to be independent of hardware device type – [46] was evaluated on a Nvidia TESLA V100, and Intel Xeon Gold 5218. Extraction attacks designed to target particular software and hardware device vulnerabilities (DS, DR) were studied across three Nvidia GPUs (TESLA V100, GTX 1080, GTX 970) and three Intel CPUs (i5-3470, i7-4770 and i7-6850k). These devices were selected to study extraction attack effectiveness when exposed to different hardware dimensions of GPU architecture (Maxwell, Pascal, Tesla), GPU Compute schedule capability, CPU generation (3rd, 4th, 6th) and CPU cache size (6MB, 8MB, 15MB). All experiments used Ubuntu 20.04.2 with CUDA 11.3, and were performed on ML frameworks PyTorch 1.11.0, and TensorFlow 1.10.0 / 2.10.0.

6.2 Datasets

Experiments leveraged four datasets selected based on their complexity (class size, image size, number of channels), and their observed impact upon API-based extraction attack on inference models [36]. Datasets include:

MNIST. [34] 60,000 training and 10,000 test greyscale images with 28x28 input size and 10 classes. Images contain white hand–written numbers on a black background.

CIFAR100. [33] 50,000 training and 10,000 test colored images with a 32x32 input size and 100 classes. Images represent photos of animals, buildings, and vehicles.

CelebA. [65] 200,000 celebrity face greyscale images with an 218x178 input size, associated with 40 attributes. We selected 10 faces out of 10,177 identities, as inclusion of this dataset is focused on investigating further attack staging described in Section 7.4.

ImageNet. [13] 14 million colored images with an 224x224 input size and 1000 classes. In our experiments, we used a subset of ImageNet providing 80,000 training and 20,000 test images (which we simply refer to as ImageNet).

Two types of datasets are used to undergo and evaluate extraction attack effectiveness. (1) *Query dataset:* A collection of inputs that an adversary can use to extract stolen classified labels from a target model. The query dataset size represents the amount of queries an adversary can perform. (2) *Testing dataset:* Used to evaluate extraction fidelity of the stolen model compared to the target model. Test sets are derived from the selected dataset test images, and thus are related to the target model trained dataset.

6.3 Target Models

Our study utilizes 21 DL model architectures [2] across three data sets described in Section 6.2, with the exception of CelebA dedicated to exploring the impact of further attack staging. Architectures selected for evaluation were chosen based on diversity of parameter size, model family, commonality within extraction literature, and also includes more modern models such as ConvNext, RegNet, and ViTB16 [15, 37, 50].

Target models were acquired via online repositories or trained locally. Online target models were sourced from TorchVision for KON and DS [39], or Keras for DR [11], which provide pre-trained ImageNet weights upon a given architecture. MNIST and CIFAR target models were trained via a transfer learning approach where pre-trained ImageNet models were re-trained to learn the new dataset. Training was performed with mini-batch size set to 10, and a cross-entropy loss function with a learning rate of 0.01 using a v100 GPU [44]. Target models were trained for 3 and 40 epochs for MNIST and CIFAR, respectively following similar training models in literature [33, 34].

6.4 Extraction Attacks

KnockOffNets (KON). We used MNIST, CIFAR100, and ImageNet as query datasets for target models. Stolen model training leveraged identical training setup in Section 6.3 with epochs set to 10, 20, and 100 for MNIST, CIFAR, and ImageNet, respectively and were selected due to differences in dataset complexity and success indifference [36]. The number of maximum queries for each attack relates to the training set size or is chosen due to overfitting with indifferent success, therefore the only reduced dataset was MNIST which used 10,000 queries, while CIFAR, and ImageNet both used their maximum training size. For the purposes of generalization, all query dataset input image sizes were transformed to 224x224. We also investigated the impact of dataset class sizes by randomly selecting classes available from the dataset to create smaller subsets which were trained across all architectures.

DeepSniffer (DS). Kernel metrics were collected using NVPROF to profile a model during a single inference similarly to Hu *et al.* [25]. Each target model was extracted 25 times to measure variation in extraction success across runs and then additionally repeated across all evaluated GPUs (GTX 970, GTX 1080, Tesla V100). This collectively totals 750 results for running DS across the system.

DeepRecon (DR). Target models were deployed within two containerized software environments. The first, identical to [24], was configured to perform 10 inferences each on 10 models, accounting for stochastic interference from the operating system. When inference begins, symbol extraction starts, and the detected symbols collected. Each model performed 10 inferences 100 times, totaling 10,000 results across per
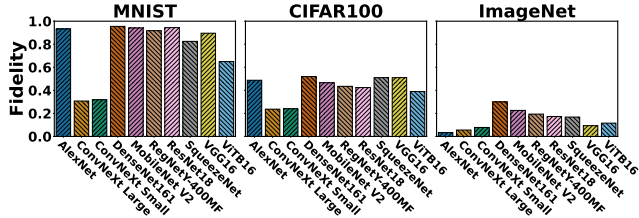

Figure 3: **KnockOffNets extraction results.** Extraction success across architectures and datasets. CSG: MNIST (7.54), CIFAR100 (79.67), ImageNet (648.99).

---

machine. Thresholds of 200 (default) were reported for all runs, as alternative thresholds (mean value using the Mastik FR-threshold function) were found to have no impact upon results. Outlined in Section 4.3, PCA was used to fingerprint the models, by using computed components to train and evaluate a KNN-classifier to classify the model architecture, and family from a given symbol result set. A model's depth and architecture could be predicted (an *exact classification*), but the predicted model family was also recorded (*family classification*). The second environment ran a version of DeepRecon compatible with TensorFlow 2.10, allowing more models to be tested. Certain cache symbols, specifically MatMul, were found to not be compatible with TF 2.10, though were not replaced to avoid modifying the attack.

6.5 Evaluation metrics

Attack success. Extraction *fidelity* is a metric is widely used within extraction literature [46, 58] to measure attack success, whereby the characteristics of the stolen and original model are directly compared by using the Top1-accuracy of predicted classified labels (KON) or architecture prediction (DS). Additional metrics of relevance collected including number of queries (KON) and model accuracy.

Complexity Measurement. To study the relationship between adversarial attack and target model complexity, we utilize two different techniques to quantify dataset and model architecture complexity. Dataset complexity was measured using *Cumulative Spectral Gradient (CSG)* [5] that projects extracted dataset features into lower dimensions and calculates class overlap using a Monte-Carlo method, capturing dataset separability, with higher values denoting higher complexity. Architecture complexity was measured by multiply-add (MAdd) [56], a technique whereby the total number of multiplication operations is computed via operator feature maps sizes within the DL model.

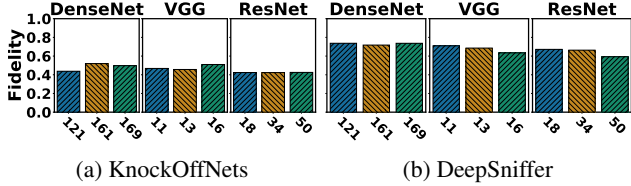[2]Appendix Table A.2 details the full model types and configurations.

Figure 4: **Architecture family depth comparison.** Fidelity variance with models of different depths/parameters using same model architecture family.

7 Extraction Attack Evaluation

7.1 KnockOffNets (KON)

KON exhibited varying success across different target model and dataset combinations as shown in Figure 3, with DenseNet161 achieving highest overall success in MNIST (0.95), CIFAR100 (0.52) and ImageNet (0.29). We identified multiple influences on attack success from model architecture, dataset complexity, class size, and number of queries.

Model architecture. We observed that target models (AlexNet, DenseNet161, VGG16) leveraging more conventional CNN architecture achieved higher success. In contrast, state-of-the-art target model architectures (ConvNeXt Small, ViTB16, RegNetY-400MF) reported lower success, with the transformer model ViTB16 exhibiting the lowest fidelity (0.0 – 0.18). As shown in Figure 4a, we determined that the number of architecture layers for target model family had minor impact, with minimal variation in extraction fidelity across families. Such architectures exhibit exceedingly complex high amount of trainable parameters and MAdd (Table A.1). Therefore, successfully extracting target models via attacks requiring exact architecture knowledge (such as KON) are increasingly difficult for models with large training requirements (queries and time). Such findings indicate that using complex architectures can intrinsically hinder adversary success without considerable effort, similarly to security methods that attempt to exceed adversary effort as a deterrent [64].

Dataset complexity. Target models using MNIST exhibited the highest attack success, with multiple architectures reporting over 0.9 fidelity, whereas ImageNet indicated the lowest attack success between 0.03 – 0.29 (Figure 3). The reason for such results is due to dataset complexity [36], whereby MNIST is least complex dataset (CSG value of 7.54) in comparison to ImageNet (CSG value 648.99). Increased dataset complexity results in more difficult class generalization and higher likelihood of overfitting [36]. Figure 5 demonstrates the impact of dataset class size on attack effectiveness. For instance, increasing ImageNet class size with DenseNet161 from 10 to 1000 resulted in reduced attack success from 0.41 to 0.29. Figure 6a and 6c depict that smaller class sizes produce higher fidelity with less queries, and additionally show that fidelity of CIFAR100 is fixed when a model is converged.

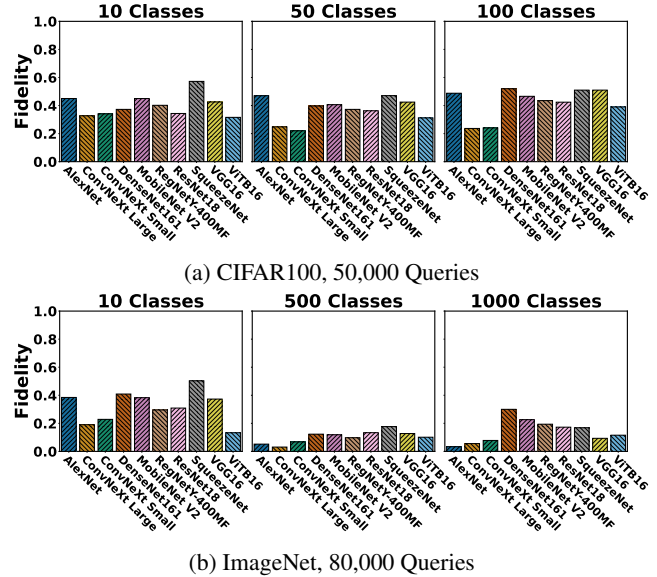(a) CIFAR100, 50,000 Queries

(b) ImageNet, 80,000 Queries

Figure 5: **Varying class sizes for KnockOffNets attack.** Datasets were reduced to a given class size and were trained via transfer learning.

Intuitively, smaller class size results in reduced dataset complexity, thus allowing a model to generalize faster with less data to achieve higher extraction success.

Query number. As provided in Figure 3, we found across all target models, the number of queries launched [10,000, 50,000, 80,000] for MNIST, CIFAR100, and ImageNet, respectively exhibited the highest impact on attack success whereby datasets of less complexity are stolen quicker. Given the training recreation technique used within KON, whereby more training data would lead (in moderation) to higher success due to greater learning generalization and diversity of data as shown in Figure 6b, also reported in [36]. Architectures and datasets of higher complexities, such as ConvNeXt upon ImageNet, require larger amount of queries for adequate extraction success.

7.2 DeepSniffer (DS)

DS also exhibited varying attack success across all evaluated architectures and DL environments. Across GPU devices, Densenet161 achieved the highest success for GTX 970 (0.71) and GTX 1080 (0.78), and ResNet18 within Tesla V100 (0.71). We determined that extraction attack success was influenced by three main factors; model architecture, ML framework, and GPU environment.

Model architecture. As shown in Figure 7, we observed that DS achieved consistently achieved high attack success across evaluated model architectures. We discovered that DS was ineffective when applied to newer models (ConvNeXt, RegNet, ViTB16) due to including operators and net-

(a) Class size (VGG16, ImageNet)

(b) Models
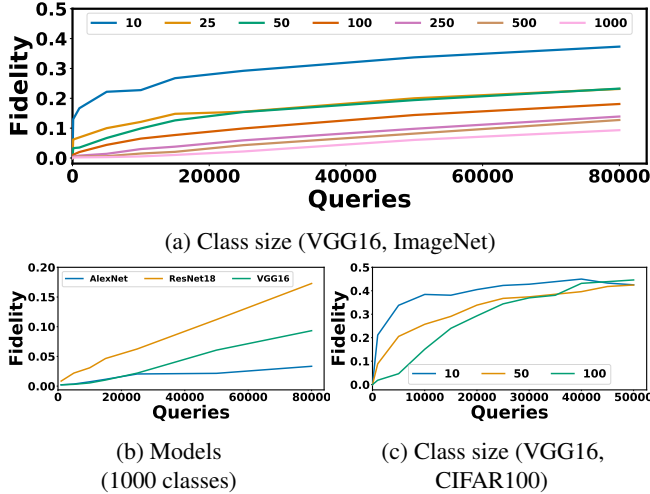(1000 classes)

(c) Class size (VGG16, CIFAR100)

Figure 6: **Varying query amounts.** KnockOffNets extraction upon ImageNet and Cifar100 across DL model architectures, various class sizes, and query amounts.

work designs not found within conventional evaluated models (ResNet, VGG, etc) [15, 37, 50]. ConvNeXt and ViTB16 both implement Gausesian Error Linear Units (GELU) as replacements to widely used Rectified Linear Units (ReLU) [22]. ViTB16 additionally uses Transformer specific operators [59], and RegNet introduces a completely new network design paradigm [50]. As such, these new operators and architectural approaches cannot be transformed into dimensions recognized within DS (see Section 4.2) which only capture standard operators within CNNs [25], limiting attack effectiveness for more sophisticated architectures. Moreover, Figure 4b demonstrates that deeper models (models with more layers) within the same family resulted in reduced fidelity for VGG and Resnet families, since models of increasing depth include more operators and increased likelihood of layer mis-classification.

ML framework. We found DS was ineffective for DL models using TensorFlow irrespective of target model architecture. From analyzing gathered profiled data across Pytorch and TensorFlow frameworks, TensorFlow generated additional kernel calls not seen within PyTorch. Thus, the increased size of profiled data results in the trained DS classifier predicting an architecture length greater than expected. The existence of such noise can be attributed to low-level framework-level optimizations when kernels execute in comparison to PyTorch. This finding indicates that DS is framework specific, and thus requires training on different frameworks to generalize extraction, and further threat model refinement to enable adversary knowledge of the system framework (Table A.4).

GPU architecture. As shown in Figure 7, we observed substantive variance in attack success across architectures for different GPUs, with GTX 970, and GTX 1080 exhibiting similar trends with slight variation. Across all GPUs, we ob-
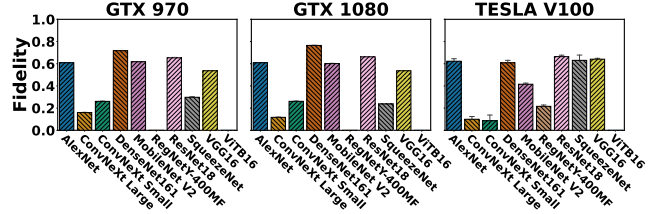

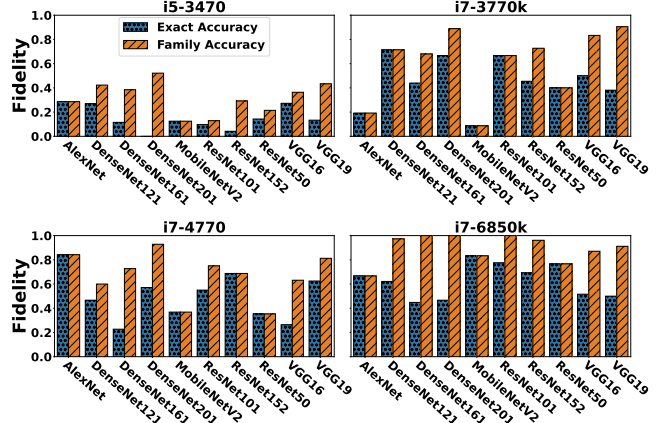Figure 7: **DeepSniffer extraction results across GPU devices and various ImageNet DL architectures.**

Figure 8: **DeepRecon model architecture & family prediction.** Classifying model family was more successful in comparison to target model classification, due to similar clustering properties.

served clear DS attack ineffectiveness when targeting newer state-of-the-art models (ConvNeXt, RegNet, ViTB16). Of particular interest, RegNetY-400MF, ConvNeXt Small and ConvNeXt Large exhibited low attack success across devices (0.12 - 0.20) and failing to extract for RegNetY-400MF. Such phenomena indicates that architecture attack susceptibility to DS is strongly affected by the GPU device. These architectural differences affect the information leakage gathered by NVPROF, with optimizations and floating-point precision varying between GPUs causing recorded kernel metrics (execution duration, read, write amounts) to change.

7.3 DeepRecon (DR)

DR demonstrated varying success across hardware platforms evaluated as shown in Figure 8. Primarily exploring TensorFlow 1.10, DenseNet (0.835) and VGG (0.766) architectures exhibited high family prediction success on all hardware tested (Figure 8), with other families showing a preference for a given CPU (AlexNet: i7-4770, MobileNet: 6850k). We noticed less distinct patterns of success across model architectures of varying depths, e.g. DenseNet depth 161 broadly being classified less accurately than 121 and 201 (Figure 8).
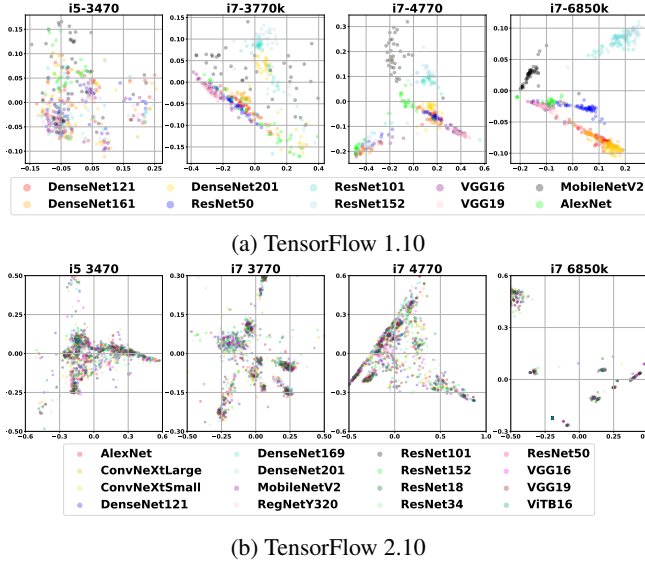
(a) TensorFlow 1.10

(b) TensorFlow 2.10

Figure 9: **Principle component analysis (PCA) for 26,000 inferences using DeepRecon across 16 models, 4 CPUs and 2 TensorFlow releases.** Clustering denotes models with similar proportions of cached operators, clearer clustering indicating similar caching behavior. PCA was used to reduce 8 detected symbols for each inference into 2 dimensions.

CPU architecture. We observed that higher performance CPUs were more vulnerable to DR, with i7-6850k achieving the highest average family classification accuracy (0.836), and i5-3470 lowest (0.316). We attribute this to cache policies and older CPUs being less responsive to timings of Flush+Reload– e.g. i5-3470 generating large but disparate symbol logs leading to a disturbed PCA result (Figure 9a). Higher performance CPUs (i7-3770k, i7-4770, i7-6850k) reported a higher effectiveness in fingerprinting and classification across model families compared to i5-3470. This is further reinforced in Figure 8, with the i5-3470, i7-4770, and i7-6850k averaging 0.316, 0.495, 0.661, and 0.836 across all model families respectively. Findings show cache size does not influence results, as Hong *et al.* [24] evaluated with a Gen4. 4MB CPU successfully, smaller than our i5-3470 (Gen3, 6MB).

Model architecture & family. As shown in Figure 9, we observed target models within model families with distinct operator traits (ResNet; residual operators, DenseNet; dense blocks) successfully fingerprinted, but overlapped with other family members. This is shown further when models were often misclassified individually but with high success within a family. Across all machines, DenseNet exact classification never exceeded 0.518 for any depth (121: 0.518, 161: 0.307, 201: 0.426), but by family averaged 0.835, similarly seen in VGG (Table A.3). This indicates that families with homogeneous operators built strong fingerprints, but using this to train classifiers for specific depths is insufficient.

TensorFlow framework TensorFlow 2.10 displayed a gen-

(a) MNIST PWCCA vs Fidelity (b) CelebA PWCCA vs Fidelity

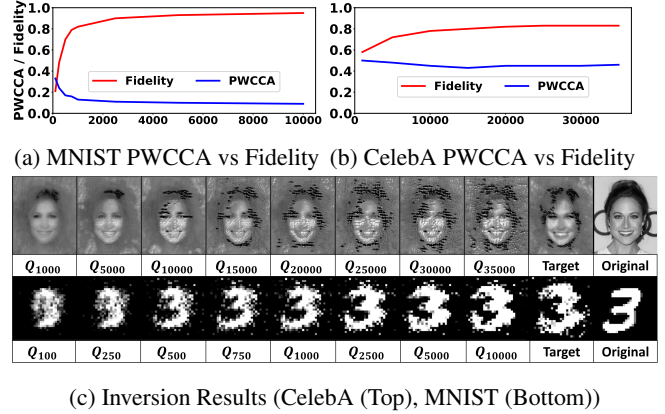(c) Inversion Results (CelebA (Top), MNIST (Bottom))

Figure 10: **Model inversion upon stolen models.** Using stolen models from KON across varying query amounts (Q_n) evaluated against target model, and original image.

eral decrease in exact and family classification accuracy across i5-3470, i7-4770 & i7-6850k systems and models, which we attribute to the missing MatMul operator decreasing the reducible dimensions for component analysis. Conversely, i7-3770k performed unexpectedly well compared to other systems, and demonstrated high accuracy on ConvNeXt Small/Large, RegNetY320, and ViTB16 (Appendix 13).

7.4 Adversarial Attack Staging

Extraction attacks have been identified as a means to stage further adversarial attacks [25, 62, 69]. Using PINCH, we conduct a case study whereby an adversary uses an extraction attack to stage a further model inversion attack.

Scenario setup. Two target models; a 3-layer and 4-layer model architecture for MNIST and CelebA, respectively, were stolen by KON. The subsequent shadow model is then exposed to a model inversion attack *MiFace* [17], whereby model information is used to generate images representative of target model classes. The MiFace attack was performed on the shadow model at various query requests for MNIST [100 – 10000] and CelebA [1000 – 35000] to evaluate MiFace attack success at different stolen model fidelity. Following the threat model in Section 3 the adversary has access to an auxiliary dataset, and partial knowledge of the target model. Thus images representative of model classes; written numbers for MNIST and random faces for CelebA, are used for image initialization [17, 21]. MiFace attack success when applied to a stolen model was evaluated by comparing generated images against images generated by the target model.

Inversion success. Observing results from Figure 10, it is apparent that even partial extraction success (0.83, 0.95) can result in successful model inversion exhibiting similar generated features comparable to the target. Specially, class features such as shape are captured to a high degree of accuracy. For

example, CelebA successfully captured dataset specific features face shape, eye and mouth positioning inline with the actual image of the class. These captured features enable the adversary to gain additional knowledge about the target models, and therefore exploit this knowledge to further augment the model inversion attack, or repeat extraction with a more tuned query set. Dataset complexity also affects inversion success. A less complex dataset such as MNIST shows highly similar images, whereas CelebA – a more complex dataset – introduces more noise due to more granular greyscale and the image containing more distinctive features [34, 65].

Extraction sensitivity. Additionally, we demonstrate MiFace upon stolen models of varying query amounts and highlight that successful inversion occurs with low query amounts and fidelity varying on dataset complexity (Figure 10c). We observed that both datasets begin to show class features early with MNIST establishing a clear shape with 500 queries and similarly CelebA at 10,000 queries. Interestingly, we see that the fidelity of the CelebA stolen model shows signs of convergence with over 25,000 queries, however displays different model inversion results despite no increase in fidelity.

Architecture similarity. To further investigate the similarity between target and stolen models, we applied Projection Weighted Canonical Correlation Analysis (PWCCA) [41] that measures similarity by calculating the distance between the activation layers of two models during inference (Figure 10a and 10b). We observed that increasing query amounts for MNIST resulted in higher fidelity and PWCCA distance to decrease, denoting high similarity. CelebA also follows this trend until 15,000 queries where the PWCCA distance was at its lowest, however additional query amounts increase the PWCCA distance despite fidelity increasing. This is due to training being a high dimensional optimization problem, whereby their exists high numbers of *Local Optimum* that can achieve similar fidelity and accuracy due to outputs have similar [2]. These local optimum can have large parameter space between them, thus exhibiting a high PWCCA distance.

8 Discussion

8.1 Key Extraction Characteristics

Within our evaluation in Section 7 we have identified multiple characteristics influencing attack success, each exhibiting a particular affinity for specific attacks (e.g. dataset complexity for KON, hardware for DR). We determined that differences within model architecture directly altered success of all attacks. As such, it is apparent that DL models appear to exhibit different resistance against certain attacks based on their model architecture characteristics. We suspect this phenomena also exists for other types of adversarial attacks. Further study of this finding would allow researchers to more effectively study and explain commonalities between adversarial attacks within complex networked systems and provide
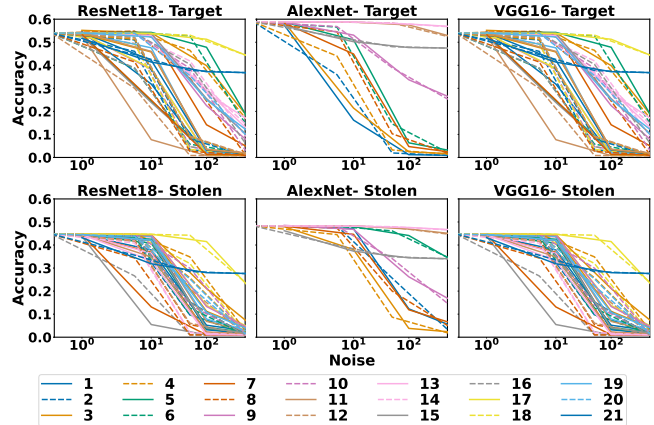

Figure 11: **Layer sensitivity to noise.** Each line represents the sensitivity of a CIFAR100 model layer to increasing magnitudes of noise, highlighting its expressive power.

practitioners the ability to focus engineering effort (validation, countermeasures, design) to secure DL models against attacks with the highest likelihood of success based on their architectural characteristics.

8.2 Further Attack Staging

From conducting experiments, we observed that even with stolen models acquired from partially successful extraction attacks can be leveraged to stage further adversarial attacks such as model inversion to attain reasonable levels of success (0.7+ fidelity). Less complex datasets such as MNIST are considerably less noisy compared to more complex datasets such as CelebA. However defined features can still be extracted by the inversion attack such as face shape, and gender (Figure 10). The ability to extract such features is especially concerning given the privacy related issues associated with specific types of models such as facial recognition, which allow an adversary to reverse engineer the classes to generate and expose images associated with real world people [17, 21]. This highlights that underlying hidden knowledge present within DL models can be extracted from stolen models, and therefore adversarial attack staging must be studied further.

8.3 Extraction Equivalency

Fidelity vs PWCCA. We observe that due to the high dimensional optimization problem existing in training networks, Fidelity and PWCCA can contrast between each other due to the existence of many local optimum (See Section 7.4). Despite not being exactly equivalent to their targets, stolen models still contain concerning information originating from the target model. This implicates that a new measurement of
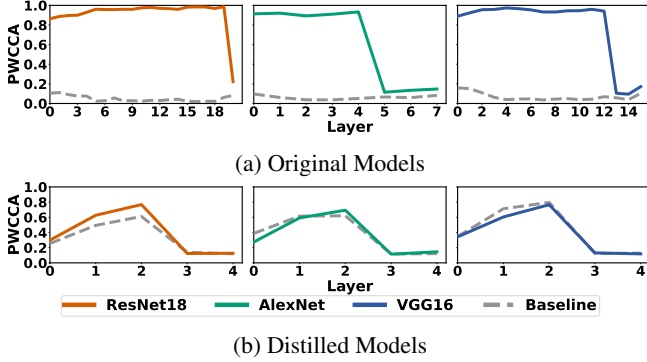
(a) Original Models

(b) Distilled Models

Figure 12: **Knowledge distillation upon stolen models.** PWCCA distance comparison of target and stolen models across ResNet18, AlexNet, and VGG16 further distilled into a 5 layer CNN [23]. Baselines computed by comparing target models with an identically trained model.

similarity is required to better understand the success of adversarial attacks, and further the creation of countermeasures.

Expressive power of models. We analyzed the expressiveness of the target and stolen model to investigate the layer sensitivity to noise by utilizing the method proposed in [51]. We compared the sensitivity of the target and stolen model to increasing magnitudes of noise to explore if the same layers of these two models exhibit the same pattern in accuracy degradation (Figure 11). Similarly to the findings within the proposed method, stolen models hold true to the statement *trained networks are more sensitive to their lower (initial) layer weights*, as earlier layers in stolen models were also most sensitive. Additionally, target and stolen models exhibit different sensitivity to noise across the majority of layers within the network, highlighting how fundamentally the models have learned differently to each other. Further understanding the difference in expressiveness would benefit the development of adversarial defences and secure DL models by providing foresight into how stolen models adapt target model knowledge into their own expressive structure.

Knowledge capture We explored how much similar knowledge a stolen model captured from a target model. Knowledge Distillation (KD) [23] was used to transfer the extracted knowledge of the target and stolen models into small distilled models, and then PWCCA is exploited to measure the representation similarities of these distilled models. Our experimental results indicate that similar captured knowledge exists between the target and stolen models. As shown in Figure 12, we distilled the target and stolen model of 3 DNNs into smaller 5 layer CNNs, achieving accuracy's stated in Table A.5. The PWCCA distance of the distilled models in Figure 12b is drastically lower compared to the original models in Figure 12a, indicating that stolen models are capable of capturing knowledge contained within a target model despite being expressively different (Figure 11).

9 Related Work

There is a growing body of research dedicated towards the study of adversarial attacks against DL model architectures and datasets within DL systems [1] [7] [8] [28] [38] [49] [52].

Extraction attack studies. Tramèr *et al.* [58] introduced the first extraction attack to extract target ML models exposed in online prediction APIs. Papernot *et al.* [47] proposed an avatar approach to extract a substitute DNN model for the purpose of generating adversarial examples. Different from [47], Joon *et al.* [45] designed an avatar based approach to train a meta-model to predict model hyperparameters. Junti *et al.* [31] developed a generic method for extracting DNN models by optimizing training hyperparameters and generating synthetic queries. Orekondy *et al.* [46] proposed a reinforcement learning based framework to improve query sample efficiency and performance. Hua *et al.* [26] first studied on reverse engineering of CNN on hardware accelerators, and investigated potential vulnerabilities in CNN accelerators in the context of model stealing. Wang *et al.* [61] provided hyperparameter stealing attacks to DL models.

Adversarial attack frameworks. Hussain *et al.* [29] presented a library allowing for black-box and label-only extraction, inference and inversion attacks on DL models. As an extended work of [29], Nicolae *et al.* [43] developed a more feature-rich library for evaluating and defending ML models to extraction, inference, inversion and poisoning attacks. Chen *et al.* [10] designed a Frank-Wolfe algorithm-based adversarial attack framework for white-box and black-box settings. Pearce *et al.* [48] provided a generic automation tool for testing the security of ML. Liu *et al.* [36] proposed a holistic risk assessment of different inference attacks against ML models and established a threat model taxonomy. In contrast to these works, we propose an end-to-end automated extraction attack framework capable of conducting an in-depth evaluation of extraction attacks across various operational scenarios and heterogeneous hardware platforms.

10 Conclusion

In this paper we have conducted an extensive empirical experimentation of extraction attack scenarios. Utilizing PINCH to rapidly design, deploy, and analyze a large number of extraction attack scenarios not yet captured in current literature, we have conducted a detailed study of extraction effectiveness against different DL system environments. We identify key insights into the fundamental understanding of adversarial security: We have (1) uncovered key extraction characteristics whereby specific model configurations exhibit strong resilience to specific attacks; (2) stolen models exhibit equivalent functionality with fundamentally different model characteristics and expressive power; and (3) demonstrated even partial extraction success enables staging of further privacy concerning adversarial attacks.

References

[1] Naveed Akhtar and Ajmal Mian. Threat of adversarial attacks on deep learning in computer vision: A survey. *Ieee Access*, 6:14410–14430, 2018.

[2] Zeyuan Allen-Zhu. Natasha 2: Faster non-convex optimization than sgd. *Advances in neural information processing systems*, 31, 2018.

[3] Battista Biggio, Igino Corona, Davide Maiorca, Blaine Nelson, Nedim Šrndić, Pavel Laskov, Giorgio Giacinto, and Fabio Roli. Evasion attacks against machine learning at test time. In *Joint European conference on machine learning and knowledge discovery in databases (ECML PKDD)*, pages 387–402. Springer, 2013.

[4] Battista Biggio and Fabio Roli. Wild patterns: Ten years after the rise of adversarial machine learning. *Pattern Recognition*, 84:317–331, Dec 2018.

[5] Frederic Branchaud-Charron, Andrew Achkar, and Pierre-Marc Jodoin. Spectral metric for dataset complexity assessment. In *IEEE/CVF Conference on Computer Vision and Pattern Recognition (CVPR)*, June 2019.

[6] Frank Buschmann, Regine Meunier, Hans Rohnert, Peter Sommerlad, Michael Stal, Peter Sommerlad, and Michael Stal. *Pattern-Oriented Software Architecture, Volume 1, A System of Patterns*, volume 1. John Wiley & Sons New York, 1996.

[7] Anirban Chakraborty, Manaar Alam, Vishal Dey, Anupam Chattopadhyay, and Debdeep Mukhopadhyay. Adversarial attacks and defences: A survey. *arXiv preprint arXiv:1810.00069*, 2018.

[8] Anirban Chakraborty, Manaar Alam, Vishal Dey, Anupam Chattopadhyay, and Debdeep Mukhopadhyay. A survey on adversarial attacks and defences. *CAAI Transactions on Intelligence Technology*, 6(1):25–45, 2021.

[9] Varun Chandrasekaran, Kamalika Chaudhuri, Irene Giacomelli, Somesh Jha, and Songbai Yan. Exploring connections between active learning and model extraction. In *USENIX Security Symposium*, pages 1309–1326. USENIX Association, 2020.

[10] Jinghui Chen, Dongruo Zhou, Jinfeng Yi, and Quanquan Gu. A frank-wolfe framework for efficient and effective adversarial attacks. In *AAAI conference on artificial intelligence*, volume 34, pages 3486–3494, 2020.

[11] François Chollet. Keras: The python deep learning library. *Astrophysics source code library*, pages ascl–1806, 2018.

[12] The MITRE Corporation. MITRE ATLAS Adversarial Attack Knowledge Base, 2022. [Online; accessed 05-Sept-2022].

[13] Jia Deng, Wei Dong, Richard Socher, Li-Jia Li, Kai Li, and Li Fei-Fei. Imagenet: A large-scale hierarchical image database. In *IEEE conference on computer vision and pattern recognition (CVPR)*, pages 248–255. Ieee, 2009.

[14] NVIDIA Developer Documentation. Cuda toolkit profiler documentation, May 2022. [Online; accessed 05-Sept-2022].

[15] Alexey Dosovitskiy, Lucas Beyer, Alexander Kolesnikov, Dirk Weissenborn, Xiaohua Zhai, Thomas Unterthiner, Mostafa Dehghani, Matthias Minderer, Georg Heigold, Sylvain Gelly, et al. An image is worth 16x16 words: Transformers for image recognition at scale. *arXiv preprint arXiv:2010.11929*, 2020.

[16] Vasisht Duddu, Debasis Samanta, D Vijay Rao, and Valentina E Balas. Stealing neural networks via timing side channels. *arXiv preprint arXiv:1812.11720*, 2018.

[17] Matt Fredrikson, Somesh Jha, and Thomas Ristenpart. Model inversion attacks that exploit confidence information and basic countermeasures. In *ACM SIGSAC conference on computer and communications security (CCS)*, pages 1322–1333, 2015.

[18] Karan Ganju, Qi Wang, Wei Yang, Carl A Gunter, and Nikita Borisov. Property inference attacks on fully connected neural networks using permutation invariant representations. In *ACM SIGSAC conference on computer and communications security (CCS)*, pages 619–633, 2018.

[19] Priya Goyal, Piotr Dollár, Ross Girshick, Pieter Noordhuis, Lukasz Wesolowski, Aapo Kyrola, Andrew Tulloch, Yangqing Jia, and Kaiming He. Accurate, large minibatch sgd: Training imagenet in 1 hour. *arXiv preprint arXiv:1706.02677*, 2017.

[20] Kaiming He, Xiangyu Zhang, Shaoqing Ren, and Jian Sun. Deep residual learning for image recognition. In *IEEE conference on computer vision and pattern recognition ((CVPR))*, pages 770–778, 2016.

[21] Zecheng He, Tianwei Zhang, and Ruby B. Lee. Model inversion attacks against collaborative inference. In *Annual Computer Security Applications Conference (ACSAC)*, page 148–162. Association for Computing Machinery, 2019.

[22] Dan Hendrycks and Kevin Gimpel. Gaussian error linear units (gelus), 2016.

[23] Geoffrey Hinton, Oriol Vinyals, Jeff Dean, et al. Distilling the knowledge in a neural network. *arXiv preprint arXiv:1503.02531*, 2(7), 2015.

[24] Sanghyun Hong, Michael Davinroy, Yiğitcan Kaya, Stuart Nevans Locke, Ian Rackow, Kevin Kulda, Dana Dachman-Soled, and Tudor Dumitraş. Security analysis of deep neural networks operating in the presence of cache side-channel attacks. *arXiv preprint arXiv:1810.03487*, 2018.

[25] Xing Hu, Ling Liang, Shuangchen Li, Lei Deng, Pengfei Zuo, Yu Ji, Xinfeng Xie, Yufei Ding, Chang Liu, Timothy Sherwood, and Yuan Xie. Deepsniffer: A dnn model extraction framework based on learning architectural hints. In *Conference on Architectural Support for Programming Languages and Operating Systems (ASPLOS)*, page 385–399, 2020.

[26] Weizhe Hua, Zhiru Zhang, and G Edward Suh. Reverse engineering convolutional neural networks through side-channel information leaks. In *ACM/ESDA/IEEE Design Automation Conference (DAC)*, pages 1–6, 2018.

[27] Ling Huang, Anthony D. Joseph, Blaine Nelson, Benjamin I.P. Rubinstein, and J. D. Tygar. Adversarial machine learning. In *ACM Workshop on Security and Artificial Intelligence (AISec)*, page 43–58, 2011.

[28] Sandy Huang, Nicolas Papernot, Ian Goodfellow, Yan Duan, and Pieter Abbeel. Adversarial attacks on neural network policies. *arXiv preprint arXiv:1702.02284*, 2017.

[29] Suha Hussain, Philip Wang, and Jim Miller. Privacyraven: Comprehensive privacy testing for deep learning, 2020.

[30] Matthew Jagielski, Nicholas Carlini, David Berthelot, Alex Kurakin, and Nicolas Papernot. High accuracy and high fidelity extraction of neural networks. In *USENIX security symposium*, pages 1345–1362, 2020.

[31] Mika Juuti, Sebastian Szyller, Samuel Marchal, and N Asokan. Prada: protecting against dnn model stealing attacks. In *IEEE European Symposium on Security and Privacy (EuroS&P)*, pages 512–527. IEEE, 2019.

[32] Ben Keller, Rangharajan Venkatesan, Steve Dai, Stephen G. Tell, Brian Zimmer, William J. Dally, C. Thomas Gray, and Brucek Khailany. Deep learning inference accelerator with per-vector scaled 4-bit quantization for transformers in 5nm. In *IEEE Symposium on VLSI Technology and Circuits (VLSI Technology and Circuits)*, pages 16–17, 2022.

[33] Alex Krizhevsky and Geoffrey Hinton. Learning multiple layers of features from tiny images. pages 32–33, 2009.

[34] Y. Lecun, L. Bottou, Y. Bengio, and P. Haffner. Gradient-based learning applied to document recognition. *Proceedings of the IEEE*, 86(11):2278–2324, 1998.

[35] Yann LeCun, Yoshua Bengio, and Geoffrey Hinton. Deep learning. *nature*, 521(7553):436–444, 2015.

[36] Yugeng Liu, Rui Wen, Xinlei He, Ahmed Salem, Zhikun Zhang, and Michael Backes. ML-Doctor: Holistic risk assessment of inference attacks against machine learning models. In *USENIX Security Symposium*, 2022.

[37] Zhuang Liu, Hanzi Mao, Chao-Yuan Wu, Christoph Feichtenhofer, Trevor Darrell, and Saining Xie. A convnet for the 2020s. In *IEEE/CVF Conference on Computer Vision and Pattern Recognition (CVPR)*, pages 11976–11986, 2022.

[38] Nag Mani, Melody Moh, and Teng-Sheng Moh. Defending deep learning models against adversarial attacks. *International Journal of Software Science and Computational Intelligence*, 13(1):72–89, 2021.

[39] Sébastien Marcel and Yann Rodriguez. Torchvision the machine-vision package of torch. In *ACM International Conference on Multimedia (MM)*, page 1485–1488. Association for Computing Machinery, 2010.

[40] Carl Meyer. Python Enhancement Proposal 405 – Python Virtual Environments, 2011. [Online; accessed 05-Sept-2022].

[41] Ari Morcos, Maithra Raghu, and Samy Bengio. Insights on representational similarity in neural networks with canonical correlation. *Advances in Neural Information Processing Systems*, 31, 2018.

[42] Hoda Naghibijouybari, Ajaya Neupane, Zhiyun Qian, and Nael Abu-Ghazaleh. Rendered insecure: Gpu side channel attacks are practical. In *ACM SIGSAC conference on computer and communications security (CCS)*, pages 2139–2153, 2018.

[43] Maria-Irina Nicolae, Mathieu Sinn, Minh Ngoc Tran, Beat Buesser, Ambrish Rawat, Martin Wistuba, Valentina Zantedeschi, Nathalie Baracaldo, Bryant Chen, Heiko Ludwig, et al. Adversarial robustness toolbox v1. 0.0. *arXiv preprint arXiv:1807.01069*, 2018.

[44] NVIDIA. Nvidia v100, Dec 2017. [Online; accessed 05-Sept-2022].

[45] Seong Joon Oh, Bernt Schiele, and Mario Fritz. Towards reverse-engineering black-box neural networks. In *Explainable AI: Interpreting, Explaining and Visualizing Deep Learning*, pages 121–144. Springer, 2019.

[46] Tribhuvanesh Orekondy, Bernt Schiele, and Mario Fritz. Knockoff nets: Stealing functionality of black-box models. In *IEEE/CVF conference on computer vision and pattern recognition (CVPR)*, pages 4954–4963, 2019.

[47] Nicolas Papernot, Patrick McDaniel, Ian Goodfellow, Somesh Jha, Z Berkay Celik, and Ananthram Swami. Practical black-box attacks against machine learning. In *ACM Asia conference on computer and communications security (AsiaCCS)*, pages 506–519, 2017.

[48] Will Pearce and Ram Kumar Shankar Siva. Ai security risk assessment using counterfit, 2021.

[49] Han Qiu, Tian Dong, Tianwei Zhang, Jialiang Lu, Gerard Memmi, and Meikang Qiu. Adversarial attacks against network intrusion detection in iot systems. *IEEE Internet of Things Journal*, 8(13):10327–10335, 2020.

[50] Ilija Radosavovic, Raj Prateek Kosaraju, Ross Girshick, Kaiming He, and Piotr Dollár. Designing network design spaces. In *IEEE/CVF conference on computer vision and pattern recognition (CVPR)*, pages 10428–10436, 2020.

[51] Maithra Raghu, Ben Poole, Jon Kleinberg, Surya Ganguli, and Jascha Sohl-Dickstein. On the expressive power of deep neural networks. In *International conference on machine learning (ICML)*, pages 2847–2854. PMLR, 2017.

[52] Kui Ren, Tianhang Zheng, Zhan Qin, and Xue Liu. Adversarial attacks and defenses in deep learning. *Engineering*, 6(3):346–360, 2020.

[53] Albert Reuther, Peter Michaleas, Michael Jones, Vijay Gadepally, Siddharth Samsi, and Jeremy Kepner. Ai accelerator survey and trends. In *IEEE High Performance Extreme Computing Conference (HPEC)*, pages 1–9. IEEE, 2021.

[54] Armin Ronacher. Welcome to Flask — Flask Documentation (2.2.x), 2022. [Online; accessed 05-Sept-2022].

[55] Ahmed Salem, Rui Wen, Michael Backes, Shiqing Ma, and Yang Zhang. Dynamic backdoor attacks against machine learning models. In *IEEE European Symposium on Security and Privacy (EuroS&P)*, pages 703–718. IEEE, 2022.

[56] Mark Sandler, Andrew Howard, Menglong Zhu, Andrey Zhmoginov, and Liang-Chieh Chen. Mobilenetv2: Inverted residuals and linear bottlenecks. In *IEEE/CVF conference on computer vision and pattern recognition (CVPR)*, pages 4510–4520, 2018.

[57] Chawin Sitawarin, Arjun Nitin Bhagoji, Arsalan Mosenia, Mung Chiang, and Prateek Mittal. Darts: Deceiving autonomous cars with toxic signs. *arXiv preprint arXiv:1802.06430*, 2018.

[58] Florian Tramèr, Fan Zhang, Ari Juels, Michael K. Reiter, and Thomas Ristenpart. Stealing machine learning models via prediction apis. In *USENIX Conference on Security Symposium*, page 601–618. USENIX Association, 2016.

[59] Ashish Vaswani, Noam Shazeer, Niki Parmar, Jakob Uszkoreit, Llion Jones, Aidan N Gomez, Łukasz Kaiser, and Illia Polosukhin. Attention is all you need. *Advances in neural information processing systems*, 30, 2017.

[60] Jordan Walke. React – A JavaScript library for building user interfaces, 2022. [Online; accessed 05-Sept-2022].

[61] Binghui Wang and Neil Zhenqiang Gong. Stealing hyperparameters in machine learning. In *IEEE symposium on security and privacy (SP)*, pages 36–52. IEEE, 2018.

[62] Xianmin Wang, Jing Li, Xiaohui Kuang, Yu an Tan, and Jin Li. The security of machine learning in an adversarial setting: A survey. *Journal of Parallel and Distributed Computing*, 130:12–23, 2019.

[63] Junyi Wei, Yicheng Zhang, Zhe Zhou, Zhou Li, and Mohammad Abdullah Al Faruque. Leaky dnn: Stealing deep-learning model secret with gpu context-switching side-channel. In *IEEE/IFIP International Conference on Dependable Systems and Networks (DSN)*, pages 125–137, 2020.

[64] Mingfu Xue, Chengxiang Yuan, Heyi Wu, Yushu Zhang, and Weiqiang Liu. Machine learning security: Threats, countermeasures, and evaluations. *IEEE Access*, 8:74720–74742, 2020.

[65] Shuo Yang, Ping Luo, Chen-Change Loy, and Xiaoou Tang. From facial parts responses to face detection: A deep learning approach. In *IEEE International Conference on Computer Vision (ICCV)*, pages 3676–3684, 2015.

[66] Yuval Yarom and Katrina Falkner. Flush+reload: A high resolution, low noise, l3 cache side-channel attack. In *USENIX Conference on Security Symposium*, page 719–732. USENIX Association, 2014.

[67] Honggang Yu, Kaichen Yang, Teng Zhang, Yun-Yun Tsai, Tsung-Yi Ho, and Yier Jin. Cloudleak: Large-scale deep learning models stealing through adversarial examples. In *Network and Distributed Systems Security Symposium(NDSS)*, 2020.

[68] Xiaoyong Yuan, Leah Ding, Lan Zhang, Xiaolin Li, and Dapeng Wu. Es attack: Model stealing against deep neural networks without data hurdles, 2020.

[69] Yuankun Zhu, Yueqiang Cheng, Husheng Zhou, and Yantao Lu. Hermes attack: Steal {DNN} models with lossless inference accuracy. In *USENIX Security Symposium)*, 2021.

[70] Fuzhen Zhuang, Zhiyuan Qi, Keyu Duan, Dongbo Xi, Yongchun Zhu, Hengshu Zhu, Hui Xiong, and Qing He. A comprehensive survey on transfer learning. *Proceedings of the IEEE*, 109(1):43–76, 2021.

A Appendix: Additional Experimental Results

In this appendix, we report additional results complimentary to experiments mentioned throughout the paper.

System	Cache (MB)		Feature Prevalence								Simplified
			convs	fcs	softms	relus	mpool	apool	merge	bias	
i5-3470	4	X	0.0003	-0.1643	-0.0583	0.6807	-0.6021	0.3475	-0.069	-0.1340	relus>mpool>apool
		Y	-0.0004	-0.4484	0.3590	-0.4292	-0.0839	0.5101	0.373	-0.2805	apool>relus>fcs
i7-4770	8	X	-0.8412	0.0808	0.0776	0.0119	0.0625	0.1082	0.5136	-0.0136	convs>merge>apool
		Y	0.3603	-0.0684	-0.0680	-0.6455	-0.0605	-0.0983	0.6524	-0.0718	merge>relus>convs
i7-6850k	15	X	-0.7878	-0.0029	-0.0038	0.5642	-0.0054	0.0044	0.2462	-0.0148	convs>relus>merge
		Y	-0.1529	0.0051	0.0001	-0.5671	-0.0118	-0.0081	0.8060	-0.0712	merge>relus>convs

Table A.1: **Hardware platforms evaluated against the DeepRecon side-channel attack, and PCA feature prevalence.** Well-fingerprinted systems i7-4770 and i7-6850k closely align on the most prevalent features (*Conv*, *Merge*, *ReLU*).
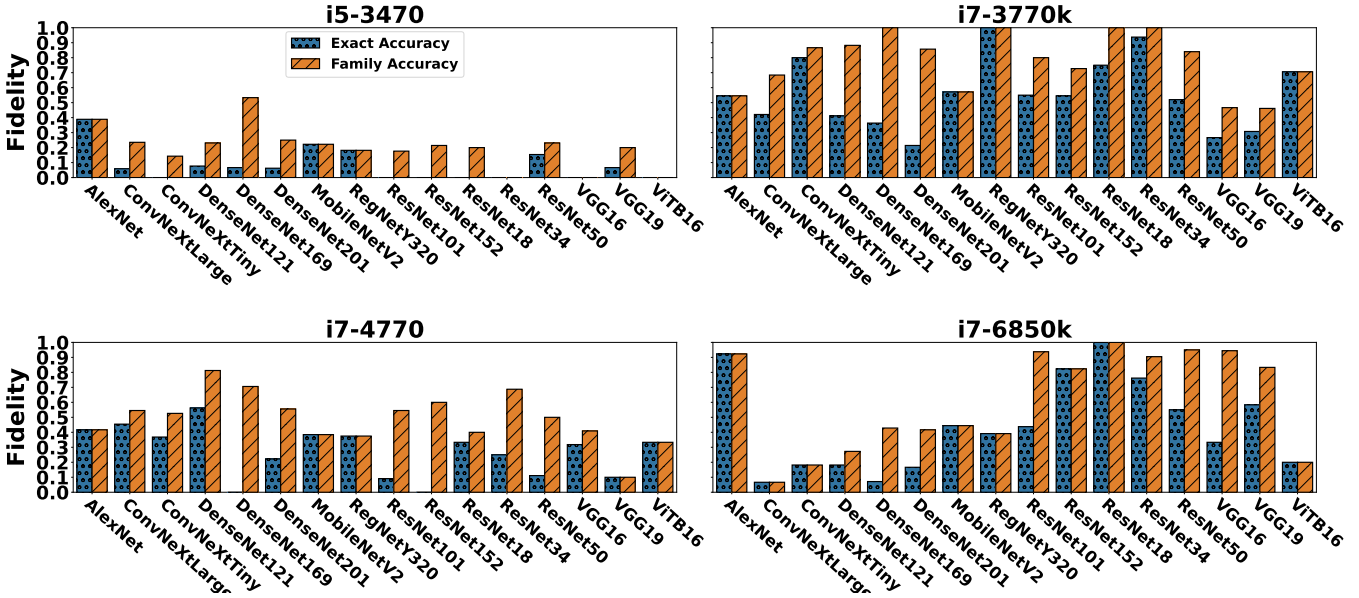

Figure 13: **DeepRecon model architecture & family prediction for TensorFlow 2.10.**

Name	Family	Parameters	GMAdd	KON	DS	DR
Alexnet	-	61.10m	0.72	Y	Y	Y
ConvNeXt_Small	ConvNeXt	50.21m	8.70	Y	Y	Y
ConvNeXt_Large		197.74m	34.40	Y	Y	Y
Densenet121		7.99m	2.88	Y	Y	Y
Densenet161	Densenet	28.68m	7.82	Y	Y	Y
Densenet169		14.14m	3.42	Y	Y	N
Densenet201		20.01m	4.37	N	N	Y
Resnet18		11.68m	1.82	Y	Y	N
Resnet34		21.79m	3.68	Y	Y	N
Resnet50	Resnet	25.55m	4.12	Y	Y	N
Resnet101		44.55m	7.85	N	N	Y
Resnet152		60.19m	11.58	N	N	Y
VGG11		132.86m	7.63	Y	Y	N
VGG13	VGG	133.04m	11.34	Y	Y	N
VGG16		138.358m	15.50	Y	Y	Y
VGG19		143.67m	19.67	N	N	Y
RegNetY-400MF	-	4.344m	0.41	Y	Y	N
SqueezeNet	-	1.248m	0.83	Y	Y	N
ViTB16	-	86.568m	11.28	Y	Y	Y
MobileNetV2	-	3.50m	0.32	Y	Y	Y
InceptionV3	-	27.161m	2.85	N	N	Y

Table A.2: **Experiment model architectures.** (KON=KnockOffNets, DS=DeepSniffer, DR=DeepRecon).

Model	Average Exact Accuracy Across All Hardware (1 d.p.)	Family	Average Family Accuracy Across All Hardware (1 d.p.)	Hardware Average Family Accuracy (1 d.p.)			
				i5-3470	i7-3770k	i7-4770	i7-6850k
AlexNet	0.50	AlexNet	0.50	0.29	0.19	**0.84**	0.67
DenseNet121	0.52						
DenseNet161	0.31	DenseNet	0.84	0.52	0.89	0.93	**1.0**
DenseNet201	0.43						
MobileNetV2	0.35	MobileNet	0.35	0.13	0.09	0.37	**0.83**
ResNet50	0.42						
ResNet101	0.52	ResNet	0.43	0.21	0.40	0.35	**0.77**
ResNet152	0.47						
VGG16	0.39	VGG	0.77	0.43	0.91	0.81	**0.91**
VGG19	0.41						

Table A.3: **DeepRecon Average Results Across Models.** Includes results collected across all runs and hardware.

Name	PyTorch	TensorFlow
VGG16	0.64	-28.76
MobileNet_V2	0.41	-3.76
ResNet50	0.57	-6.96
Inception_V3	0.13	-10.56

Table A.4: **DeepSniffer Framework Comparison PyTorch vs TensorFlow.** Recorded fidelity between actual and predicted architecture from PyTorch and TensorFlow frameworks. TensorFlow returns unusable results.

Name	Target	Stolen	Distilled Target	Distilled Stolen
ResNet18	0.54	0.45	0.35	0.36
AlexNet	0.59	0.48	0.36	0.35
VGG16	0.61	0.44	0.36	0.35

Table A.5: **Distillation Accuracy Results.** Accuracy scores based on CIFAR100 test set upon original and distilled target and stolen models.